Metal-insulator transition of the two-band Hubbard model in infinite dimension and its relevance to a strongly correlated electron system: $NiS_{2-x}Se_x$

H. Watanabe
Department of Applied Physics, Stanford University, Stanford, California 94305

S. Doniach
Department of Applied Physics and Department of Physics, Stanford University, Stanford, California 94305

(Received 7 April 1997; revised manuscript received 11 September 1997)

We report a study of metal-insulator transition of a strongly correlated two-band Hubbard model using a dynamical mean-field theory approach. We find that the Mott transition appears at half filling even at $T=0$ in contrast to the one-band Hubbard model. The transition is characterized by the development of a ''Kondo-like'' peak near Fermi level. We also find a signature of the coexistence of metallic and antiferromagnetic phases from the study of the single-particle Green's function and the magnetic long-range order due to the superexchange coupling between the correlated electrons. We then suggest the relevance of our results to the metal-insulator transition and the recent angle-resolved photoemission measurements of $NiS_{2-x}Se_x$. We also study the effect of carrier doping and the comparison of our findings with the experimental results suggests the possible importance of departures from stoichiometry associated with the Se substitution. The relevance of our results to high-temperature superconductivity is also discussed. [S0163-1829(98)02507-7]

I. INTRODUCTION

The discovery of high-temperature superconductors has stimulated a renewed interest in strongly correlated electron systems. Transition-metal compounds have been the subject of extensive study both theoretically and experimentally in the quest of the key to the mechanism of high-T_c superconductivity. A pyrite compound $NiS_{2-x}Se_x$ is one of the examples where simple band theory fails to work and the effect of electron-electron correlation is of primary importance. At sufficiently low temperatures, increasing the selenium fraction drives a transition from an antiferromagnetic insulating state to an antiferromagnetic metallic state[1–5] without any apparent structural distortion. (In principle, the substitution of Se does not change the number of valence electrons.) The absence of any apparent symmetry breaking of crystal structure at the metal-insulator (MI) transition renders this material an attractive candidate for a model system to study the evolution of electron degrees of freedom during the transition neglecting the lattice degrees of freedom. The antiferromagnetic long-range order persists into the metallic phase. The existence of a well-defined phase transition between an antiferromagnetic insulating phase and an antiferromagnetic metal phase has been one of the key motivations in these studies. Recently, $NiS_{2-x}Se_x$ was investigated by the angle-resolved photoemission technique[6] and the photoemission cross section was found to develop a narrow peak at the Fermi level as the material reached the verge of the MI transition. This narrow feature was attributed to many-body effects in analogy to the Kondo resonance.[6]

In this paper we report a theoretical study of this class of quantum phase transition using the dynamical mean-field theory approach.[7] In this approach a many-fermion system is mapped onto a system of self-consistently embedded impurities where the time dependence is represented through the local dynamics of the impurities. This theory becomes exact in the $d=\infty$ limit and captures nontrivial aspects of physics of strongly correlated systems in finite dimensions, which have been difficult to address by preexisting theories.[7] The one-band Hubbard model at half filling constrained in the paramagnetic phase was shown[8] to exhibit a correlation-induced MI transition (Mott transition) as a function of on-site Coulomb repulsion. The onset of the transition was found to be signaled by the appearance of a resonant peak at the Fermi level inside the gap. However, the onset of a spin-density-wave induced gap completely preempts the Mott transition to a metallic state and it is necessary to introduce frustration into the one-band model in order to suppress the onset of magnetic order and recover the Mott mechanism for the transition.[9] In particular, in order to restore the Mott mechanism at $T=0$, the one-band model needs to be fully frustrated, which may not be realistic to describe a real crystal. From a more realistic point of view, most of the transition-metal compounds contain nonmetals as well as transition metals, and nonmetal degrees of freedom are frequently integrated out in favor of a simplified effective model. Therefore, one may be tempted to ask if a more rigorous treatment of nonmetal degrees of freedom may cause the Mott mechanism (i.e., a charge-transfer type[10]) in a true ground state and what the magnetic structure of the system during the transition is, particularly in connection to $NiS_{2-x}Se_x$. In order to address this question, we therefore have approached the problem by studying the strongly correlated two-band Hubbard model,[11] and studied simultaneously the evolution of the single-particle Green's function and the development of magnetic long-range order as a function of both charge-transfer gap and hole doping. The MI transition of the two-band Hubbard model in the paramagnetic phase has previously been studied in the $d=\infty$ limit,[12] and a crossover diagram similar to the scheme obtained by Zaanen, Sawatzky, and Allen[10] was reproduced. However, the evolution of the single-particle Green's function in the course of the MI transition and the possible occurrence of a broken-symmetry antiferromagnetic phase are addressed for the two-band Hubbard model in the $d=\infty$ limit in the present work.

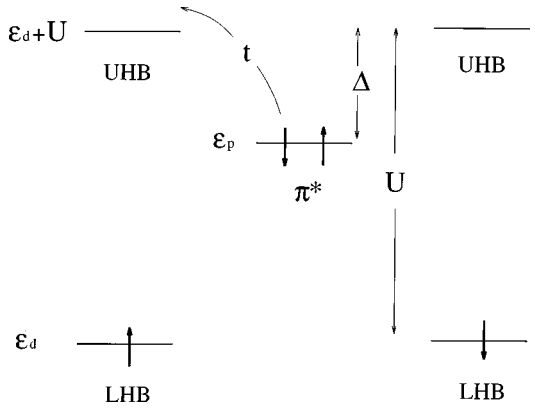

FIG. 1. Schematic describing the parameters used in the Hamiltonian (1). UHB and LHB: Upper and lower Hubbard bands.

We then address the relevance of our numerical results to the real system. In particular, we compare our results with $NiS_{2-x}Se_x$, focusing on the two phenomena that appear to characterize this class of materials, namely, a metal-insulator transition in the presence of antiferromagnetic order and the development of a peak at the Fermi level at the MI transition. We also suggest a possibility of hole doping in this material that might occur experimentally as a result of the creation of S and Se vacancies. In Appendix A, we briefly describe how $NiS_{2-x}Se_x$, which has a complicated pyrite structure, can be fit to the two-band Hubbard model after some simplifications. We finally suggest some similarities between our results and high-T_c cuperates.

II. MOTT MECHANISM IN THE TWO-BAND HUBBARD MODEL

The two-band Hubbard model we study in this paper takes the following familiar form:

$$H=-\sum_{\langle i,j\rangle,\sigma} t(\hat{d}^{\dagger}_{i\sigma}\hat{p}_{j\sigma}+\hat{p}^{\dagger}_{i\sigma}\hat{d}_{j\sigma})+(\epsilon_d-\mu)\sum_{i\sigma}\hat{n}_{d,i\sigma}$$
$$+(\epsilon_p-\mu)\sum_{i\sigma}\hat{n}_{p,i\sigma}+U\sum_{i}\hat{n}_{d,i\uparrow}\hat{n}_{d,i\downarrow}, \qquad (1)$$

where $\hat{d}^{\dagger}_{i\sigma}$ ($\hat{p}^{\dagger}_{i\sigma}$) is the creation operator of a d (p) electron with spin σ at site i and $\hat{n}_{d,i\sigma}$ ($\hat{n}_{d,i\sigma}$) is a number operator of d (p) electrons with spin σ at site i. The electron hopping is considered only between the nearest-neighbor d and p sites and electron-electron correlation is assumed to be appreciable only on the d sites. The energy parameters are chosen to be $\epsilon_d<\epsilon_p<\mu<\epsilon_d+U$, which represents the materials we are interested in, including high-T_c cuprates and $NiS_{2-x}Se_x$. Note that we only consider one d orbital per unit cell although Ni ions are expected to be in a d^8 state. We discuss this simplifying approximation in Appendix A. A charge-transfer gap is defined as $\Delta\equiv\epsilon_d+U-\epsilon_p$ (Fig. 1). Note, however, that a case of $\epsilon_d<\mu<\epsilon_p<\epsilon_d+U$ (i.e., $\Delta\equiv\epsilon_p-\epsilon_d$) is related to the above case through a particle-hole symmetry. We study the MI transition of this model, as a function of charge-transfer gap Δ and hole doping δ [$\equiv 1.5-\Sigma_\sigma(n_{d\sigma}+n_{p\sigma})$]. The Hamiltonian (1) and its effective Hamiltonian[13] have been studied extensively in the context of high-temperature superconductivity.

We now qualitatively argue that the Hamiltonian (1) may contain the necessary ingredients to cause the Mott mechanism in the presence of antiferromagnetic order. In the study of the one-band Hubbard model at half filling in $d=\infty$,[7] the transition from the insulating to the Fermi liquid phase may be identified in a naive sense as the onset of electron hopping when the dimensionless parameter $\tilde{t}=t/U$ becomes of $O(1)$. Since the effective antiferromagnetic coupling of nearest-neighbor spins for the one-band Hubbard model is of order $J=t^2/U$ and the dimensionless parameter $\tilde{J}=J/U$ is also of $O(1)$, the antiferromagnetic long-range order in the insulating phase competes with the onset of the Fermi-liquid phase and can inhibit it by completely gapping the Fermi surface unless suppressed by magnetically frustrating interactions.[10]

In a two-band Hubbard model at finite U, there is an extra degree of freedom as the effective bandwidth of the hybridized d band is given by $W=t^2/\Delta$ that corresponds to the second-order virtual hopping of electrons between the nearest-neighbor d and p sites. Thus the metal-insulator criterion becomes $W/\Delta=O(1)$. However, in the competition between formation of a nonmagnetic Fermi-liquid ground state, which may be characterized by a Kondo energy $E_{\rm Kondo}\cong W\exp(-W/J)$, and a magnetic metallic ground state characterized by a Ruderman-Kittel magnetic energy $E_{\rm RK}\cong J^2/W$, where the effective antiferromagnetic coupling between d spins and the effective noninteracting electron bath is of order $J=t^2U/(U-\Delta)\Delta$,[14] the magnetic energy can win for large Δ such that W/J is larger than a critical threshold value while the onset of the Fermi-liquid phase is controlled by W/Δ.[15]

This suggests the following qualitative scenario. Close to a zero temperature and for a sufficiently large charge-transfer gap $W<\Delta$, quantum fluctuations of both charge and spin are suppressed and the system is expected to be in the antiferromagnetic insulating phase. As Δ is gradually decreased, the onset of the Fermi-liquid phase sets in through quantum charge fluctuations at $\Delta=\Delta_c=O(t)$. However, W/J [$\cong(U-\Delta)\Delta^2/Ut^2$] may still be above the critical value at which the Kondo screening spin fluctuations destroy the magnetic phase, so the system passes into a metallic antiferromagnetic state. It should be noted that the precise balance between the value of Δ below which the system becomes metallic and above which it remains antiferromagnetic is a subtle issue that will depend on the details of the model considered. We show below that this condition is satisfied in the $d\to\infty$ limit assuming certain details about how the two-band model is mapped onto this limit. This need not necessarily be true for more general models.

III. CONSTRUCTION OF THE SELF-CONSISTENCY CONDITION IN THE INFINITE-DIMENSIONAL LIMIT

In this section, we illustrate how we map the two-band Hubbard model onto a particular configuration. The Hamiltonian (1) has already been a subject of study in the infinite-dimensional limit, and it was shown[12] that the lattice in which d (p) states occupy the A (B) sublattice has a well-defined infinite-dimensional limit. (See, however, recent Ref. 16.) In this work, we will further break the translational sym-

metry to allow for the effects of superexchange coupling between the spins on d sites via p sites. The superexchange coupling remains finite in $d=\infty$ since it is of the order of $t^4\sim d^{-2}$ ($t\sim d^{-1/2}$, $d=$dimensionality), and the number of pairs of d sites that couple through superexchange interaction is of the order of d^2. (Equivalently, connectivity instead of dimensionality may be used.) We will consider a Bethe lattice for which the one-band Hubbard model has already been shown to exhibit qualitatively the same physics as on a hypercubic lattice in the infinite-dimensional limit.[17] Consequently, two inequivalent p sites are created on the lattice, but this can be remedied by introducing a multiband system (Fig. 2).

The set of equations that constitutes our formalism in the $d=\infty$ limit consists of the local problem of d sites:

$$S_{\rm imp}^{A[B]}=-\sum_{\sigma}\int_0^\beta\int_0^\beta d\tau\, d\tau'\,\hat{d}_\sigma^{A[B]\dagger}(\tau)D_{o\sigma}^{A[B]-1}(\tau-\tau')\hat{d}_\sigma^{A[B]}(\tau')-U\int_0^\beta d\tau[\hat{n}_\uparrow^{A[B]}(\tau)-\tfrac{1}{2}][\hat{n}_\downarrow^{A[B]}(\tau)-\tfrac{1}{2}], \tag{2}$$

$$D_\sigma^{A[B]}(\tau-\tau')=\frac{\mathrm{Tr}\{\hat{d}_\sigma^{A[B]\dagger}(\tau)\hat{d}_\sigma^{A[B]}(\tau')e^{-S_{\rm imp}^{A[B]}(D_o^{A[B]})}\}}{\mathrm{Tr}\{e^{-S_{\rm imp}^{A[B]}(D_o^{A[B]})}\}}=\frac{\int\mathcal{D}\hat{d}^{A[B]\dagger}\mathcal{D}\hat{d}^{A[B]}\hat{d}_\sigma^{A[B]\dagger}(\tau)\hat{d}_\sigma^{A[B]}(\tau')e^{-S_{\rm imp}^{A[B]}(D_o^{A[B]})}}{\int\mathcal{D}\hat{d}^{A[B]\dagger}\mathcal{D}\hat{d}^{A[B]}e^{-S_{\rm imp}^{A[B]}(D_o^{A[B]})}} \tag{3}$$

and the self-consistently condition in Fourier space:

$$D_{o\sigma}^{A}(i\omega)^{-1}=i\omega-\epsilon_d+\mu-\frac{U}{2}-t^2P_\sigma^B(i\omega), \tag{4}$$

$$D_{o\sigma}^{B}(i\omega)^{-1}=i\omega-\epsilon_d+\mu-\frac{U}{2}-t^2P_\sigma^A(i\omega), \tag{5}$$

$$P_\sigma^{A}(i\omega)^{-1}=i\omega-\epsilon_p+\mu-t^2D_\sigma^A(i\omega), \tag{6}$$

$$P_\sigma^{B}(i\omega)^{-1}=i\omega-\epsilon_p+\mu-t^2D_\sigma^B(i\omega), \tag{7}$$

where $D_{o\sigma}^{A[B]}$ is a bare Green's function of the d site of type $A[B]$ and spin σ, and $P_\sigma^{A[B]}$ is a total Green's function for p site of type $A[B]$. It may be more illuminating to eliminate the P's and write the resulting equations as

$$D_{o\sigma}^{A}(i\omega)^{-1}=i\omega-\epsilon_d+\mu-\frac{U}{2}-\frac{t^2}{i\omega-\epsilon_p+\mu-t^2D_\sigma^B(i\omega)},$$

$$D_{o\sigma}^{B}(i\omega)^{-1}=i\omega-\epsilon_d+\mu-\frac{U}{2}-\frac{t^2}{i\omega-\epsilon_p+\mu-t^2D_\sigma^A(i\omega)},$$

which reveals the bipartite relation between D_σ^A, and D_σ^B. Note that d spins only couple to d spins of the opposite types and hence no magnetic frustration.

We solve Eqs. (2)–(7) self-consistently. Given a noninteracting Green's function $D_{o\sigma}^{A[B]}$, we solve the impurity problem (2) and (3) numerically using the quantum Monte Carlo (QMC) algorithm of Hirsch and Fye[18,17] to calculate a total Green's function $D_\sigma^{A[B]}$. The self-consistency Eqs. (4)–(7) generate new noninteracting Green's functions $D_{o\sigma}^{A[B]}$. The above steps are iterated until convergence is achieved. We then use the maximum entropy (ME) method to obtain an analytically continued real-time Green's function. Our criteria for convergence is the convergence of the the location and the relative heights and widths of the characteristic peaks calculated using ME. Normally, three to four iterations will be sufficient away from MI transition, while ten or more iterations may be needed close to the MI transition.

In the algorithm of Hirsch and Fye, the local action $S_{\rm imp}$ is discretized along the imaginary time axis and bilinearized in the fermion operators by the discretized Hubbard-Stratonovich transformation using the Ising variables:[19]

$$\begin{aligned}S_{\rm imp}\approx&-\sum_{l,l'=1}^{N}(\Delta\tau)^2\sum_\sigma\hat{d}_\sigma^\dagger(l)D_{o\sigma}^{-1}(l-l')\hat{d}_\sigma(l')\\&-\frac{\lambda}{2}\sum_{l=1}^{N}\Delta\tau\sum_{\mu(l)=\pm1}\mu(l)[\hat{n}_{d\uparrow}(l)-\hat{n}_{d\downarrow}(l)]\\=&-\sum_{l,l'=1}^{N}(\Delta\tau)^2\sum_\sigma\hat{d}_\sigma^\dagger(l)D_{o\sigma}^{-1}(l-l')\hat{d}_\sigma(l')\\&-\sum_{l=1}^{N}\Delta\tau\sum_{h(l)=\pm\lambda}h(l)m_z(l),\end{aligned} \tag{8}$$

where $\beta=\Delta\tau N$, $\cosh(\lambda)=\exp(\frac{1}{2}\Delta\tau U)$, $m_z(l)\equiv[\hat{n}_{d\uparrow}(l)-\hat{n}_{d\downarrow}(l)]/2$, and $h(l)\equiv\lambda\mu(l)$. N is the number of time slices, $\mu(l)$ is a time-dependent Ising variable that takes values of $+1$ or -1, and $m_z(l)$ is the z component of the local spin of the Ni-e_g site. Equation (8) implies that $h(l)$ can be regarded as an effective local magnetic field that fluctuates and takes on the discrete values $+\lambda$ and $-\lambda$. That is, the system of interacting fermions is mapped onto that of free electrons under the influence of the self-consistently determined effective field that couples to the charge degrees of freedom and the fluctuating discrete magnetic field that couples to the spin degrees of freedom. The thermal average of $h(l)$ is given as

$$\langle h^{A[B]}\rangle=\int_0^\beta d\tau\, h_{A[B]}(\tau),$$

$$h_{A[B]}(\tau)=\frac{\mathrm{Tr}\{h^{A[B]}(\tau)e^{-S_{\rm imp}^{A[B]}(D_o^{A[B]})}\}}{\mathrm{Tr}\{e^{-S_{\rm imp}^{A[B]}(D_o^{A[B]})}\}},$$

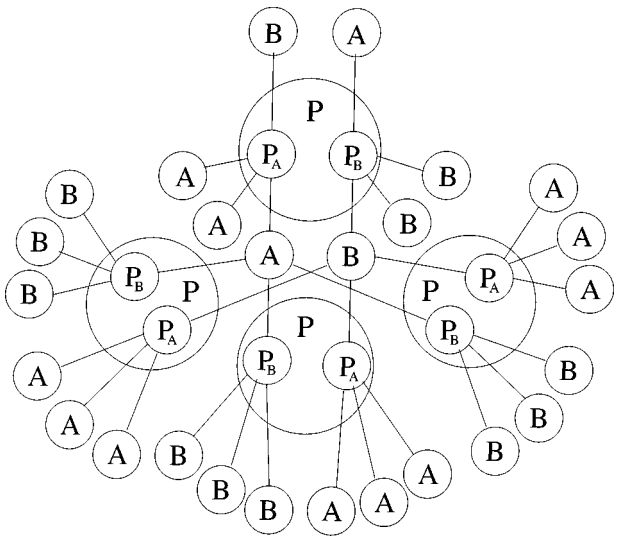

FIG. 2. Two-component Bethe lattice. Note that all the P sites are topologically equivalent.

and is numerically calculated by QMC algorithm. Whenever $\langle h^{A[B]} \rangle$ converges to a finite value, this implies that the QMC tries to break the symmetry between up-spin and down-spin and a d site acquires a tendency to prefer either one of the spin configurations. This is analogous to the slow fluctuations that occur in the local-moment regime of the Kondo problem below the Kondo temperature: however, here we have a lattice problem rather than an impurity problem so that the system sustains a true symmetry breaking. In the local moment regime, the QMC can be biased towards a particular spin sector by properly initializing the noninteracting Green's function for the input. Therefore, once the antiferromagnetism sets in, the self-consistency Eqs. (4)–(7) produce new noninteracting Green's functions in such a way that the QMC is biased to break the spin symmetry in an alternative fashion between A and B sublattices. (Since the QMC spontaneously breaks the spin symmetry in the local-moment regime, we do not need to explicitly bias the system towards a broken symmetry phase. The mechanism of biasing is implicit in the algorithm of the QMC.) Then, $\langle h^{A[B]} \rangle$ as well as $D_\sigma^{A[B]}$ correspondingly acquires a staggered nature:

$$\langle h^A \rangle \simeq -\langle h^B \rangle,$$

$$D_\sigma^A(\tau=0) \simeq D_{-\sigma}^B(\tau=0) \quad \text{or} \quad n_{d\sigma}^A \simeq n_{d-\sigma}^B,$$

which we identify as the signature of the onset of antiferromagnetism. In a preliminary study of the one-band Hubbard model, we found coexistence of metallic and insulating phases for sufficiently low temperatures near the metal-insulator transition, indicating a first-order nature for the transition. Therefore, in the two-band case, we also examined the coexistence of metallic and insulating solutions.

In this work, all the energy levels are measured with respect to ϵ_d and scaled in units of the bare bandwidth of a Bethe lattice $D(=2t)$, i.e., $D=1(t=0.5)$ and $\epsilon_d=0$. In case of the charge-transfer MI transition, the evolution of the single-particle Green's function is studied as a function of charge-transfer gap, $\Delta(\equiv U-\epsilon_p)$, for a fixed β and total

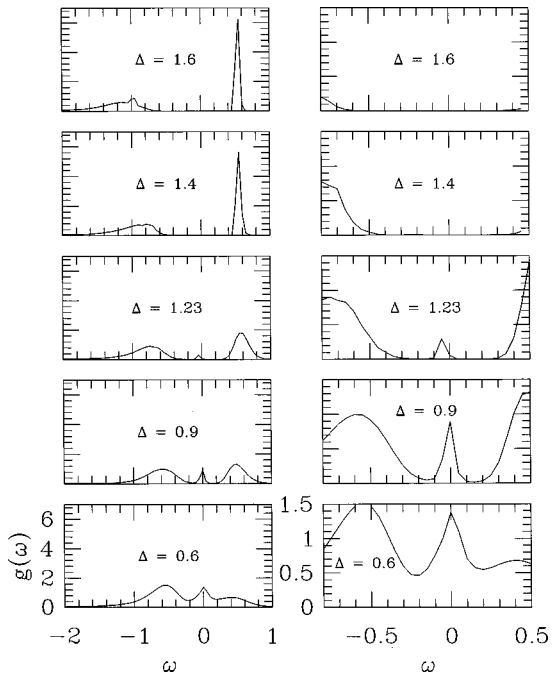

FIG. 3. The evolution of the single-particle Green's function as a function of charge-transfer gap for $\beta=32$, $U=4$. The graphs on the right side are rescaled to show near-ϵ_F features. The occupied sector is mostly of p character and the unoccupied sector of d character.

number of valence electrons, $n_{\rm tot}[\equiv\Sigma_\sigma(n_{d\sigma}+n_{p\sigma})]$. Since we cannot directly control the value of $n_{\rm tot}$, μ must be tuned to achieve a fixed value of $n_{\rm tot}$ for each Δ. In case of a doping-induced MI transition, the single-particle Green's function is studied as a function of $n_{\rm tot}$ although in practice μ is tuned to vary $n_{\rm tot}$. In order to ensure that the model can represent a charge-transfer insulator, we chose $U=4(U/D=U/2t=4)$. With this value of U, QMC can be performed down to reasonably low temperatures with a fair level of numerical accuracy and computer time. Although $U=4$ may not be a precise value for $NiS_{2-x}Se_x$, a fair qualitative success of our results suggests that our arguments will not be modified in a qualitative manner if an exact value of U is chosen. Once U is fixed, a critical value of Δ at which a charge-transfer MI transition occurs is uniquely determined.

IV. RESULTS AND ANALYSIS

A. Charge-transfer metal-insulator transition

We studied the charge-transfer MI transition for $\beta=16$ and 32. In Fig. 3, we plot the evolution of the single-particle Green's function for $\beta=32$, calculated using the metallic initial Green's function. For $\beta=32$, we found the signature of coexistence of a metallic and an insulating solutions for $1.0\leqslant\Delta\leqslant1.23$, indicating the first-order nature of the transition. A true transition is expected to occur somewhere in this region. Figure 4 shows an example of coexisting solutions for $\Delta=1.23$. The MI transition is signaled by the appearance of a narrow peak at the Fermi level (ϵ_F) inside the charge-transfer gap with its center slightly below ϵ_F. A relatively sudden broadening of the upper Hubbard band (UHB) can be observed at the MI transition and is due to the onset of the

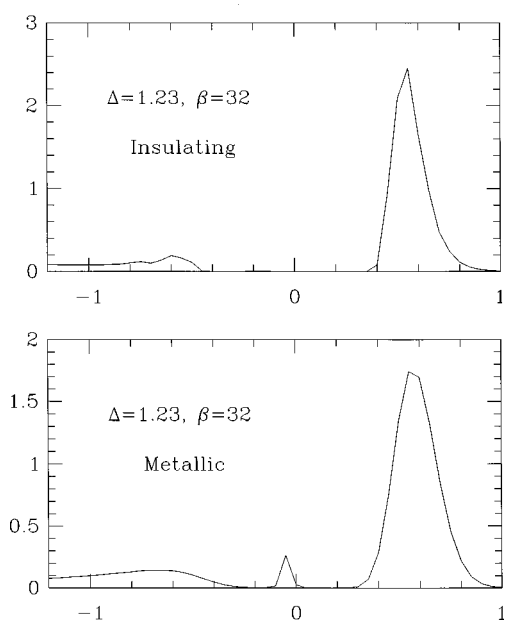

FIG. 4. Coexisting solutions of the single-particle Green's function for a metallic and an insulating phase for $\beta=32$ and $\Delta=1.23$.

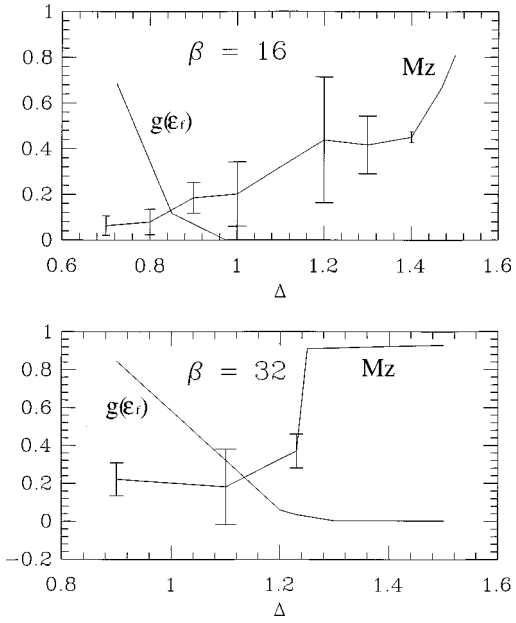

FIG. 5. Staggered magnetization and the spectral weight at ϵ_F vs charge-transfer gap for $\beta=32,\ 16$.

virtual second-order electron hopping. The appearance of the peak slightly below ϵ_F is probably due to the broken particle-hole symmetry in contrast to the Mott transition of the one-band Hubbard model at half filling where the particle-hole symmetry enforces the peak to appear strictly on ϵ_F. The projective self-consistent approach[20] may be able to address the further details of the evolution of the single-particle Green's function near ϵ_F. For $\beta=16$, we found no evidence of coexistence of a metallic and an insulating solutions and the MI transition occurs in a crossover fashion where the charge-transfer gap closes continuously without the signature of the appearance of a peak at ϵ_F within our numerical resolution. The spectral function at ϵ_F starts to acquire a sizable weight around $\Delta\simeq 1.0$. We also plot the staggered magnetization $M_z=S_z^A-S_z^B=(D_\uparrow^A-D_\downarrow^A)-(D_\uparrow^B-D_\downarrow^B)$ and the spectral weight at ϵ_F, $g(\epsilon_F)$ [Figs. 5(a) and 5(b)]. For $\beta=32$, M_z starts to decrease rapidly upon approaching the MI transition, whereas, for $\beta=16$, M_z decreases rather monotonically and no apparent anomaly at the MI transition was observed. Note that for both cases, M_z remains finite even after $g(\epsilon_F)$ becomes sizable and the antiferromagnetism persists inside the Fermi-liquid phase. In Fig. 6, we plot the single-particle Green's function at half filling for a fixed charge-transfer gap ($\Delta=0.9$) as a function of temperature. Note that as the temperature is raised, a Kondo-like peak disappears and a spectral weight at the Fermi level is suppressed. Since $g(\epsilon_F)$ remains finite at $\beta=16$, it is unclear whether this suppression corresponds to the temperature-driven MI transition. However, the above results still imply the existence of a temperature-driven MI transition for $1.0\leqslant\Delta\leqslant 1.23$ depending on where the true transition occurs at $\beta=32$, i.e., from a low-temperature metallic phase to a high-temperature insulating phase. Later, we argue that it is legitimate to have this kind of temperature-driven MI transition.

B. Doping-induced metal-insulator transition

We chose $(\beta,\Delta)=(16,\ 1.6)$ for which the undoped system can be characterized as an antiferromagnetic insulator by our calculation. We present the results for the case of hole doping in Fig. 7. In the case of electron doping, the MI transition is driven by the continuous shift of the UHB towards ϵ_F and no apparent peak was observed within our numerical resolution. A peak may be expected to appear at lower temperatures due to the reduced thermal broadening, although the calculation will be numerically expensive. Again, the projective self-consistent approach may be a more suitable way to study the details. Figure 7 illustrates the effect of hole doping on the charge-transfer insulator. Note that a peak develops upon doping on top of the valence band

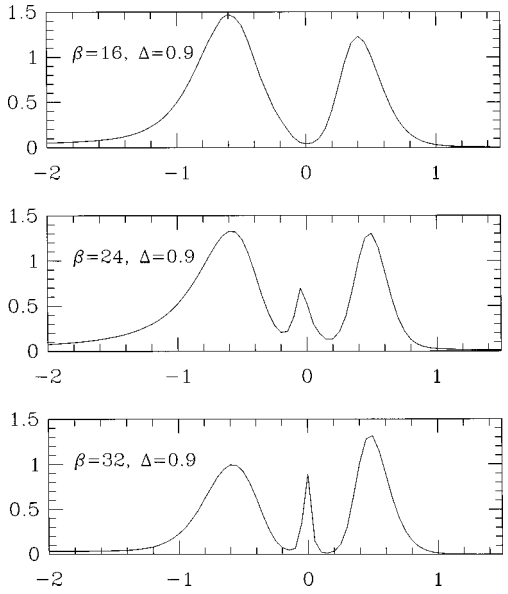

FIG. 6. Single-particle Green's functions at half filling for a fixed charge-transfer gap ($\Delta=0.9$) and varying temperatures.

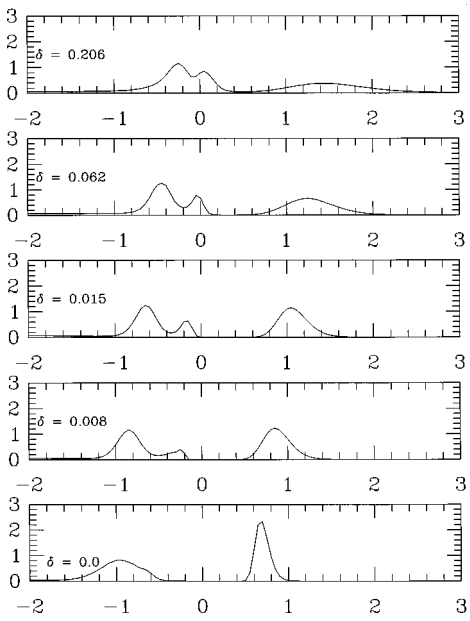

FIG. 7. The evolution of the single-particle Green's function as a function of hole doping for $\beta=16$, $\Delta=1.6$, and $U=4$. The occupied sector is mostly of p character and the unoccupied sector of d character.

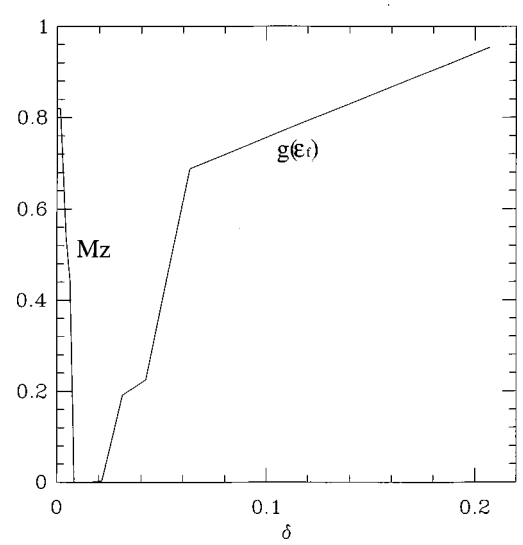

FIG. 8. Staggered magnetization and the spectral weight at ϵ_F vs hole doping for $\beta=16$, $\Delta=1.6$, and $U=4$.

below the Fermi level even before $g(\epsilon_F)$ acquires a sizable weight. As the doping is increased further, the peak grows and shifts towards ϵ_F, and $g(\epsilon_F)$ starts to become sizable at around $\delta_c \sim 0.03$. Also, the UHB broadens and, unlike the charge-transfer MI transition, shifts upward. M_z and $g(\epsilon_F)$ are plotted on Fig. 8. The effect of doping on the antiferromagnetic long-range order is rather dramatic. In contrast to the charge-transfer MI transition, the antiferromagnetism disappears immediately upon doping before $g(\epsilon_F)$ becomes sizable and no evidence was found for the coexistence of a metallic character and an antiferromagnetic long-range order.

V. DISCUSSION

As we speculated based on a qualitative argument, the two-band Hubbard model in $d=\infty$ was found to exhibit a charge-transfer MI transition from an antiferromagnetic insulator to an antiferromagnetic metal in contrast to the one-band Hubbard model at half filling where the MI transition occurs at finite temperatures from a paramagnetic metal to an antiferromagnetic insulator as a function of U. The transition was found to be of first-order character at sufficiently low temperature and becomes continuous at higher temperatures. We expect this trend will persist qualitatively when U is increased from $U=4$, although the location of the critical point may change. However, it will be interesting to ask how the nature of the charge-transfer MI transition, especially at $T=0$, is modified if U is decreased from $U=4$ but remains sufficiently large for the model to represent a charge-transfer insulator.

As discussed earlier, the above difference between the one-band and the two-band model is expected to come from the separation of the two mechanisms in the two-band Hubbard model, namely, the onset of a Fermi-liquid phase (through quantum fluctuations of the charge degrees of freedom) and the destruction of magnetic long-range order (through Kondo quantum fluctuations of the spin degrees of freedom) due to the presence of correlationless sites that mediate the superexchange coupling between the two strongly correlated states. We find the effect of the presence of the correlationless sites may be manifested in a different way. The presence of correlationless sites renders the system relatively insensitive to the choice of the initial, noninteracting Green's function compared with the one-band Hubbard system. This difference can be understood from the self-consistency equations. Even if we start with an extremely localized noninteracting Green's function, since it has to be *filtered* through the self-consistency equation twice, it acquires more renormalization and damping before it is supplied as an input for QMC. In the case of the one-band Hubbard model,[9] the Green's function has to go through the self-consistency equation only once before it is supplied as an input for the next QMC. Note that if there is no electron hopping, the self-consistency equations simply produce the noninteracting Green's function of the atomic limit that has a simple pole at the atomic level and if the electron hopping becomes finite, renormalization and damping will complicate the structure of noninteracting Green's functions. Put in different terms, the self-consistency equations of the two-band Hubbard model are less capable of distinguishing metallic from insulating solutions for a given set of parameters. In fact, in our preliminary study of the one-band Hubbard model, we found evidence of their coexistence for $\beta=16$ near the MI transition, whereas no apparent signature of this coexistence was found for the two-band Hubbard model at the same temperature.

At half filling, near the charge-transfer MI transition, we also found the implication of the temperature-driven MI transition from an antiferromagnetic metal at low temperature to an antiferromagnetic insulator at high temperature. This transition may be rationalized naively in terms of an entropy argument. In the localized phase, a low-lying excitation is an antiferromagnetic spin wave whose entropy grows as T^3 (similar to acoustic phonons), whereas in the delocalized

phase, a main contribution to the entropy at low temperatures is expected to come from the Fermi-liquid part that grows linear in T. Therefore, given that the ground state is a delocalized phase, as the temperature is raised, the entropy term in free energy will eventually favor the localized phase. (See Appendix B for more detailed arguments.) We also found qualitative differences between the charge-transfer and doping-induced MI transition in the manner that the single-particle Green's function evolves during the transition. For the charge-transfer MI transition, at sufficiently low temperatures, a narrow peak develops at ϵ_F *inside* the gap and the UHB broadens rapidly at the MI transition due to the onset of the virtual electron hopping. For the doping-induced MI transition, a preformed peak below ϵ_F continuously shifts towards ϵ_F and the UHB broadens and shifts upward during the MI transition.

We find that despite some crucial simplifications, our numerical results for the charge-transfer MI transition of the two-band Hubbard model qualitatively fit to the MI transition of $NiS_{2-x}Se_x$ with Se substitution identified as the reduction of the charge-transfer gap (Appendix A) and that this yields a proper account of the evolution of a narrow peak in the presence of antiferromagnetic order resulting from superexchange coupling between the Ni d electrons in both the insulating and metallic phases. Also, our results illustrated in Fig. 6 and qualitative arguments given in Appendix B suggest the existence of the temperature-dependent MI transition near the phase boundary and qualitatively match the experimental results.[6] However, there is one apparent discrepancy between our results (Fig. 6) and the experimental data of the evolution of angle-resolved photoemission cross section as a function of temperature.[8] In the experimental data, there remains a sizable cross section near (presumably below) ϵ_F even in the insulating phase, which is not apparent in Fig. 6. Moreover, the evolution of angle-resolved photoemission cross section as a function of Se fraction has also been found to develop a noticeable weight near (presumably below) ϵ_F in the insulating phase,[21] which is not apparent in Fig. 3, either. The appearance of cross section near ϵ_F in the insulating samples cannot be understood within our model if we assume that the effect of Se substitution is just to decrease a charge-transfer gap, but can be explained if we take into account the possibility that Se substitution causes hole doping by creating S/Se vacancies. Our results for the doping-induced MI transition suggest the development of spectral weight below ϵ_F in the insulating phase (Fig. 7). From this point of view, we can give an interpretation to the temperature-dependent angle-resolved photoemission measurement that a sudden shift of the near-ϵ_F feature is caused by the disappearance of the weight due to the charge-transfer mechanism (i.e., ''Kondo-like'' resonance) and the remainder of the weight is due to the hole-doping effect. However, if both charge-transfer and hole-doping effects are present, it may raise the question of which mechanism is a driving force for the MI transition. Since an antiferromagnetic order is expected to persist during the MI transition and our result illustrated in Fig. 8 suggests that an antiferromagnetic order is unlikely to persist across the doping-induced MI transition, our model favors the charge-transfer mechanism as a main cause for the MI transition. Although a theoretical explanation of the phase diagram of $NiS_{2-x}Se_x$ at a quantitative level will require a more sophisticated model that treats the complication of this material more rigorously, our results seem to suggest that the dynamical mean-field theory approach is a promising theory to study a strongly correlated electron system.

Finally, it is tempting to point out the relevance of our results to high-T_c cuprates. Our results show a phenomenology that is analogous to that of the cuprates from zero-doping to the overdoped region at sufficiently low temperature at a qualitative or even semiquantitative level. We show that a finite amount of doping $\delta_c \sim 0.03$ is necessary for the system to acquire a sizable weight at ϵ_F and that the antiferromagnetism disappears before the spectral weight at ϵ_F becomes sizable. However, it is difficult to tell within our numerical resolution whether the charge gap remains strictly zero for $\delta \leqslant \delta_c$. In the case of the one-band Hubbard model *in the paramagnetic phase*, the quasiparticle peak appears at ϵ_F upon doping.[21] Detailed study of the effect of carrier doping on both the one-band and the two-band Hubbard systems with the consideration of the broken symmetry phase using the projective approach will be necessary to answer the above question. In order to further clarify the relevance of these models to high-T_c superconductivity, calculations with more applicable values of the parameters (U and Δ) and perhaps more parameters (t_{pp}, U_{pd}, etc.) with the consideration of the anomalous components of the Green's function may be desirable.

In conclusion, we found that the two-band Hubbard model in infinite dimension can predict the Mott transition including $T=0$. The transition as a function of charge-transfer gap is characterized by a development of a Kondo-like peak at the Fermi level in the presence of antiferromagnetic long-range order. This result qualitatively captures the main features of the MI transition of $NiS_{2-x}Se_x$ despite the crucial simplifications necessary to model this system with the two-band Hubbard model. The study of doping effects suggests the possibility of the occurrence of carrier doping in the course of Se substitution. Also, our results seem to be relevant to the understanding of the disappearance of antiferromagnetic long-range order in the high-T_c cuprates as a function of doping. Further calculations in a relevant parameter range using a more powerful numerical approach will be desirable to pursue this conclusion for the cuprates.

ACKNOWLEDGMENTS

We thank Z-X Shen and Anne Matsuura for many stimulating discussions. We thank Nejat Bulut for the generous donation of the maximum entropy program. We acknowledge the NSF for support through Grant No. DMR9418964 and through the Center for Materials Research at Stanford University, and the San Diego Supercomputer Center for a grant of computer time.

APPENDIX A: A MODEL HAMILTONIAN FOR $NiS_{2-x}Se_x$

A pyrite, NiS_2, is an insulator and orders antiferromagnetically below the Néel temperature $T_N \simeq 40$ K. The crystal belongs to the space group $T_h^6(Pa3)$ and can be conveniently regarded as a rocksalt structure consisting of Ni^{2+} ions and S_2^{2-} dimers. Ni^{2+} has six nearest-neighbor S^- that form an octahedron with Ni^{2+} at its center. To the simplest approximation, the crystal field will split the Ni-d levels into a lower

set of threefold degenerate levels (t_{2g}) and an upper set of twofold degenerate levels (e_g) where the t_{2g} orbitals are occupied and the e_g orbitals are half filled. $3p$ orbitals of S_2^{2-} dimers will split into bonding (σ,π) and antibonding (σ^*,π^*) states where σ, π, and π^* are occupied and σ^* is unoccupied. The physics of the MI transition in Ni compounds is complicated by the twofold degeneracy of the e_g orbitals. In principle, a Hund's rule coupling must be introduced in order to favor a spin-1 pairing of the d electrons. In preliminary studies we have found that the dynamics of the Hund's rule coupling when introduced in a rotationally invariant way leads to a minus sign problem in the quantum Monte Carlo calculations. For this reason, we have focused on a simplified model in which the degeneracy of the e_g states is neglected. Despite this simplification, our results still show the essential qualitative features found in $NiS_{2-x}Se_x$ so that we believe the correct inclusion of the Hund's rule coupling would not change our conclusions in a qualitative way. Therefore, a model Hamiltonian may be constructed from half-filled e_g states of Ni $3d$ and filled π^* of S_2 $3p$ (Ref. 6) as

$$H=-\sum_{\langle i,j\rangle,\sigma} t(\hat{d}^{\dagger}_{i\sigma}\hat{p}_{j\sigma}+\hat{p}^{\dagger}_{i\sigma}\hat{d}_{j\sigma})+(\epsilon_d-\mu)\sum_{i\sigma}\hat{n}_{d,i\sigma}$$

$$+(\epsilon_p-\mu)\sum_{i\sigma}\hat{n}_{p,i\sigma}+U\sum_{i}\hat{n}_{d,i\uparrow}\hat{n}_{d,i\downarrow},$$

where $d^{\dagger}_{i\sigma}(p^{\dagger}_{i\sigma})$ is the creation operator of an $e_g(\pi^*)$ electron with spin σ at site i and $\hat{n}_{d,i\sigma}(\hat{n}_{d,i\sigma})$ is a number operator of $e_g(\pi^*)$ electrons with spin σ at site i. The electron hopping is considered only between the nearest-neighbor Ni and S_2 and only the on-site Coulomb repulsion on Ni is assumed to be appreciable. The undoped material NiS_2 has a charge-transfer gap $\Delta(\equiv\epsilon_d+U-\epsilon_p)$ between the occupied π^* band and the empty e_g band and is expected to correspond to the parameter region $t\ll\Delta$ for which the ground state of the Hamiltonian (1) is a charge-transfer insulator.[12] In this work, we restrict ourselves to two cases where Se substitution either decreases Δ by increasing an overlap matrix between $3p$ orbitals in a dimer[6] or causes hole doping by creating S/Se vacancies (see, however, Ref. 22). Our numerical results thus provide an interpretation of the experimental phenomena measuring the effects of Se substitution on NiS_2.

APPENDIX B: TEMPERATURE DEPENDENCE OF THE PHASE BOUNDARY BETWEEN ANTIFERROMAGNETIC METALLIC AND INSULATING PHASES

In the antiferromagnetic insulating phase, at sufficiently low temperatures, the leading temperature-dependent term of a free energy $F_I(T)$ is expected to come from the Goldstone mode that is the antiferromagnetic spin wave. Therefore, at low temperatures,[23]

$$F_I(T)\simeq F_I(0)-\frac{\pi^2 n_{\rm spin}(k_BT)^1}{720\sqrt{3}(JS)^3},$$

where $n_{\rm spin}$ is the density of spins. On the other hand, in the antiferromagnetic metallic phase, the leading term in a free energy $F_M(T)$ is expected to come from the Fermi-liquid character. Therefore,

$$F_I(T)\simeq F_M(0)-\frac{\pi^2 g(\epsilon_F)(k_BT)^2}{3}.$$

The condition of phase boundary,

$$F_I(T)=F_I(M)$$

gives the transition temperature T_t,

$$T_t=\sqrt{t_1+\sqrt{t_1^2+t_{\delta F}}},$$

where

$$t_1=\frac{120\sqrt{3}g(\epsilon_F)(JS)^3}{n_{\rm spin}k_B^2},$$

$$t_{\delta F}=\frac{720\sqrt{3}(JS)^3[F_I(0)-F_M(0)]}{\pi^2 n_{\rm spin}k_B^4}.$$

Thus, assuming $\Delta_c-\Delta\sim F_I(0)-F_M(0)$ near the MI transition at $T=0$, the slope of the metal-insulator phase boundary near $T=0$ behaves as

$$\left.\frac{\partial T_t}{\partial\Delta}\right|_{\Delta=\Delta_c,\ T=0}\sim-\frac{\sqrt{n_{\rm spin}}}{k_B(g(\epsilon_F)JS)^{3/2}}\sim-S^{-3/2}.$$

This implies that increasing the magnitude of S will make the antiferromagnetic insulating phase more stable as we raise the temperature, and the slope of the phase boundary is suppressed (i.e., the temperature-driven MI transition becomes more well defined). This implies that a temperature-driven MI transition under consideration should be more easily observed in a degenerate system such as $NiS_{2-x}Se_x$.

[1] H. S. Jarrett, R. J. Bouchard, J. L. Gillson, G. M. Jones, S. M. Marcus, and J. F. Weiher, Mater. Res. Bull. **8**, 877 (1973).

[2] G. Czjzek, J. Fink, H. Schmidt, G. Krill, M. F. Lapierre, P. Panissod, F. Gautier, and C. Robert, J. Magn. Magn. Mater. **3**, 58 (1976).

[3] S. Sudo and T. Miyadai, J. Phys. Soc. Jpn. **54**, 3934 (1985).

[4] S. Sudo, J. Magn. Magn. Mater. **114**, 57 (1992).

[5] F. Gautier, G. Krill, M. F. Lapierre, P. Panissod, C. Robert, G. Czjzek, J. Fink, and H. Schmidt, Phys. Lett. **53A**, 31 (1975).

[6] A. Y. Matsuura, Z. X. Shen, D. S. Dessau, C. H. Park, T. Thio, J.

W. Bennett, and O. Jepsen, Phys. Rev. B **53**, R7584 (1996).
[7] A. Georges and G. Kotliar, Phys. Rev. B **45**, 6479 (1992); V. Janis and D. Vollhardt, Int. J. Mod. Phys. B **6**, 283 (1992). For a comprehensive review of a dynamical mean-field theory, see A. Georges, G. Kotliar, W. Krauth, and M. J. Rozenberg, Rev. Mod. Phys. **68**, 13 (1996).
[8] X. Y. Zhang, M. J. Rozenberg, and G. Kotliar, Phys. Rev. Lett. **70**, 1666 (1993).
[9] M. J. Rozenberg, G. Kotliar, and X. Y. Zhang, Phys. Rev. B **49**, 10 181 (1994).
[10] J. Zaauen, G. A. Sawatzky, and J. W. Allen, Phys. Rev. Lett. **55**, 418 (1985).
[11] V. Emery, Phys. Rev. Lett. **58**, 2794 (1897); C. Varma, S. Schmitt-Rink, and E. Abrahams, Solid State Commun. **62**, 681 (1987).
[12] A. Georges, G. Kotliar, and W. Krauth, Z. Phys. B **92**, 313 (1993); M. Caffarel and W. Krauth, Phys. Rev. Lett. **72**, 1545 (1994).
[13] F. C. Zhang and T. M. Rice, Phys. Rev. B **37**, 3759 (1988).
[14] J. R. Schrieffer and P. A. Wolff, Phys. Rev. **149**, 491 (1966).
[15] S. Doniach, Phys. Rev. B **35**, 1814 (1987).
[16] P. Lombardo, M. Avignon, J. Schinalian, and K.-H. Bennemann, Phys. Rev. B **54**, 5317 (1996).
[17] M. Jarrel, Phys. Rev. Lett. **69**, 169 (1992); T. Pruschke, D. L. Cox, and M. Jarrel, Phys. Rev. B **47**, 3553 (1993).
[18] J. E. Hirsch and R. M. Fye, Phys. Rev. Lett. **56**, 2521 (1986).
[19] J. E. Hirsch, Phys. Rev. B **28**, 4059 (1983).
[20] G. Moeller, Q. Si, G. Kotliar, M. Rozenberg, and D. S. Fisher, Phys. Rev. Lett. **74**, 2082 (1995); D. S. Fisher, G. Kotliar, and G. Moeller, Phys. Rev. B **52**, 17 112 (1995).
[21] A. Y. Matsuura and Z. X. Shen (private communication).
[22] A. Husmann, D. S. Jin, Y. V. Zastavker, T. F. Rosenbaum, X. Yao, and J. M. Honig, Science **274**, 1874 (1996).
[23] See, for example, C. Kittel, *Quantum Theory of Solids*, 2nd revised printing (Wiley, New York, 1987).